

Athermalization Design of Dual-Field-of-View Long Wavelength Infrared Optical System

Chen Jianfa^{1,2} Wang Helong^{1,2} Liu Xin² Pan Zhifeng²

¹ Science and Technology on Electro-Optical Control Laboratory, Luoyang, Henan 471009, China
² Luoyang Institute of Electro-Optical Equipment, Aviation Industry Corporation of China, Luoyang, Henan 471009, China

Abstract A design study of athermalization of switchable dual-field-of-view optical systems for $7.7 \sim 9.7 \mu\text{m}$ is presented. With the axial motion of a lens group, a result of dual-field-of-view infrared optical system is achieved. In order to meet a wide environmental temperature range, the optical passive athermalization is used to eliminate the thermal effect in optical systems by correctly assembling different optical materials. The final optical designs along with their modulation transfer function (MTF) and root-mean-square (RMS) radius are presented, showing excellent imaging performance in dual fields-of-view at the temperature range between $-60 \text{ }^\circ\text{C}$ and $+70 \text{ }^\circ\text{C}$.

Key words optical design; infrared optical system; passive optical athermalization; dual field-of-view

OCIS codes 220.4830; 110.3080; 280.6780

双视场长波红外光学系统无热化设计

陈建发^{1,2} 王合龙^{1,2} 刘欣² 潘枝峰²

¹ 光电控制技术重点实验室, 河南 洛阳 471009
² 中国航空工业集团公司洛阳电光设备研究所, 河南 洛阳 471009

摘要 设计了一个无热化双视场长波红外光学系统, 工作波段 $7.7 \sim 9.7 \mu\text{m}$ 。通过轴向移动一组透镜实现红外系统双视场设计, 为了满足光学系统大温度范围工作的需求, 采用光学被动无热化的设计方法, 通过合理分配光学元件材料, 利用不同材料的热差特性来消除整个光学系统的热离焦, 实现了红外光学系统的无热化设计。像质评价结果表明, 光学系统在全温度范围内 ($-60 \text{ }^\circ\text{C} \sim +70 \text{ }^\circ\text{C}$) 双视场成像质量好, 接近衍射极限。

关键词 光学设计; 红外光学系统; 光学被动无热化; 双视场

中图分类号 TN216 **文献标识码** A **doi**: 10.3788/LOP49.122204

1 Introduction

In the application of space cameras, the environmental temperature range will change widely, and in the optical system, the refractive indices, surface radii, thicknesses of lenses and distances between lenses change with the temperature, so it is hard to keep the same performance in all the temperature range.

Athermalization is the correction of this effect of these changes with temperature. There are several mechanical and optical methods, active and passive, available to accomplish athermalization.

1) Mechanical passive method. The basic principle behind this approach is to passively modify the axial position of a lens or lens group in order to compensate for the image shift caused by temperature change. This movement is achieved by natural expansion or contraction of mechanical components. However, for germanium this type of correction by such metal as aluminum does not provide sufficient movement.

2) Mechanical active method. A lens or lenses are moved axially either manually or, preferably, by electromechanical means. This is particularly useful in zoom lenses where the required athermalization movements differ with magnification change.

3) Optical passive method. It is possible to select a combination of optical materials that will minimize the focus shift over a limited temperature range. For simultaneous correction of achromatism and athermalization at least three

收稿日期: 2012-08-13; 收到修改稿日期: 2012-09-16; 网络出版日期: 2012-10-19

作者简介: 陈建发(1987—), 男, 硕士研究生, 主要从事光学设计方面的研究。E-mail: ly471141@hotmail.com

导师简介: 王合龙(1965—), 男, 博士, 研究员, 主要从事光电系统总体设计方面的研究。E-mail: huqnwpu007@163.com

optical materials are required. By solving the basic equations for power, achromatism and athermalization, the relative power for each material can be derived^[1,2].

The first method is not commonly used for its special requirement of materials. The second solution increases the complexity. Optical passive athermalization is more attractive in the cases requiring lower weight and smaller volume^[3~7]. In this paper, optical passive athermalization is used to eliminate the thermal effect in the dual-field-of-view long wavelength infrared optical system.

2 Athermalization

It is possible to solve achromatism and athermalization at the same time with three infrared materials by solving the following simultaneous equations:

$$\begin{cases} \phi = \frac{1}{f} = \frac{1}{h_1} \sum_{i=1}^k h_i \phi_i \\ \omega = \frac{1}{h_1^2 \phi} \sum_{i=1}^k h_i^2 \omega_i \phi_i = 0 \\ \theta = \frac{1}{h_1^2 \phi} \sum_{i=1}^k h_i^2 \theta_i \phi_i = -\alpha \end{cases} \quad (1)$$

where h_i is the height of the paraxial marginal ray, α is the linear expansion of the mounting material, ω is the chromatic coefficient, and θ is the thermal coefficient^[8].

Athermalizing, or eliminating the thermal focus shift, is analogous to correcting the chromatic aberration of the system; it requires at least two materials with different properties^[9,10]. To correct chromatic aberration, we utilize different Abbe V -values; for athermalization we need different T -values. If we can find an appropriate combination of V - and T -values, we can simultaneously correct both the thermal and chromatic conditions. The properties of several materials suitable for use in the 7.7~9.7 μm wavelength region are listed in Table 1^[1,8].

Table 1 Thermal and chromatic properties of common infrared materials in the 7.7~9.7 μm wavelength region

Material	Thermal coefficient / ($10^{-5}/^\circ\text{C}$)	Chromatic coefficient $\omega/10^{-4}$
Ge	13.22	14.86
Amtir1	2.93	15.04
ZnS	3.57	11.15
ZnSe	3.03	28.42

3 Design example

As an example of the results of optical passive athermalization method, a dual field-of-view long wavelength infrared optical system is designed. The requirements of specification are shown in Table 2.

Table 2 Specification of the system

Parameter	Value
Wavelength / μm	7.7~9.7
Focal length / mm	100/300
Field-of-view (FOV) / ($^\circ$)	6/2
Pixel number of detector	256 \times 256
Pitch of detector / mm	0.020
F number	2
Athermalization range / $^\circ\text{C}$	-60~70

The detector has a cold shield, so the lens exit pupil has to be placed on it. Usually, for long focal lengths, the lenses for cooled detectors are constituted of two parts: a “primary lens” and an optical relay.

The relay is used to conjugate the entrance pupil on the detector cold shield to reduce “primary lens” size in order to

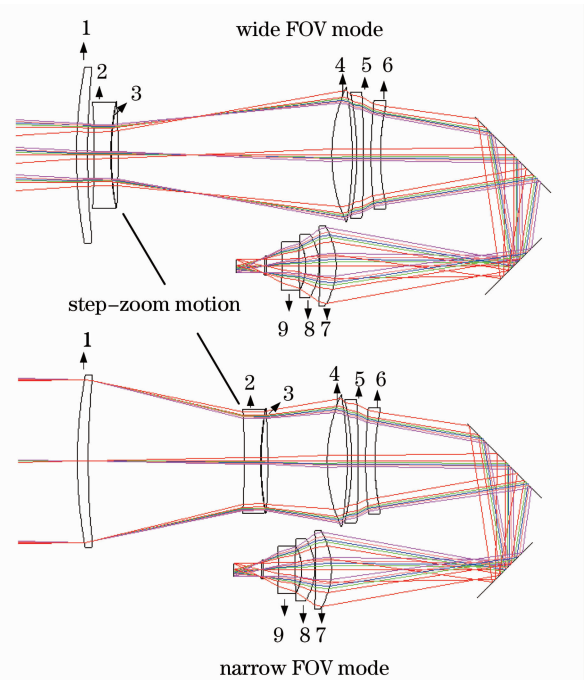


Fig. 1 Optical layout

minimize the cost, weight and volume of the system.

With the axial motion of a lens group (lenses 2 and 3), the optical system can be step-zoomed. The optical layout is shown in Fig. 1.

Lenses 1, 2, 6 and 8 are made of Ge. All concave surfaces have aspherical profiles except lens 1 and the first concave surface of lens 2.

Lenses 3, 4, and 7 are made of Amtir1 (all spherical profiles).

Lenses 5 and 9 are made of ZnS. The concave surface of lens 5 has aspherical profile.

The total transmittance T through an optical system after absorption losses is expressed by

$$T_s = \exp(-\sigma x), \quad (2)$$

where σ is the absorption coefficient and x is the distance travelling through optical elements^[1].

The optical system includes four Ge lenses, three Amtir1 lenses, two ZnS lenses and two mirrors.

The absorption coefficient of Ge is about 0.03 cm^{-1} , the total thickness of the material is 3.2 cm; the absorption coefficient of Amtir1 is about 0.005 cm^{-1} , the total thickness of the material is 3.9 cm; the absorption coefficient of ZnS is about 0.08 cm^{-1} , the total thickness of the material is 1.8 cm; the transmittance of single lens and mirror is about 98%. So, the transmission of the optical system is about

$$\tau = (0.98)^{11} \times \exp(-0.03 \times 3.2 - 0.005 \times 3.9 - 0.08 \times 1.8) \approx 0.618.$$

Making reference to Fig. 1, the deviations of the rays on each optical surface are small. These small deviations are "driven" during optimization to have low sensitive mountings and manufacturing tolerances.

The optical system optimization is carried on using CODEV. The modulation transfer functions (MTF) of the system are shown in Fig. 2. The MTF at the temperature range of $-60 \text{ }^\circ\text{C} \sim +70 \text{ }^\circ\text{C}$ is more than 0.5 at the Nyquist frequency (18 lp/mm) for every FOV.

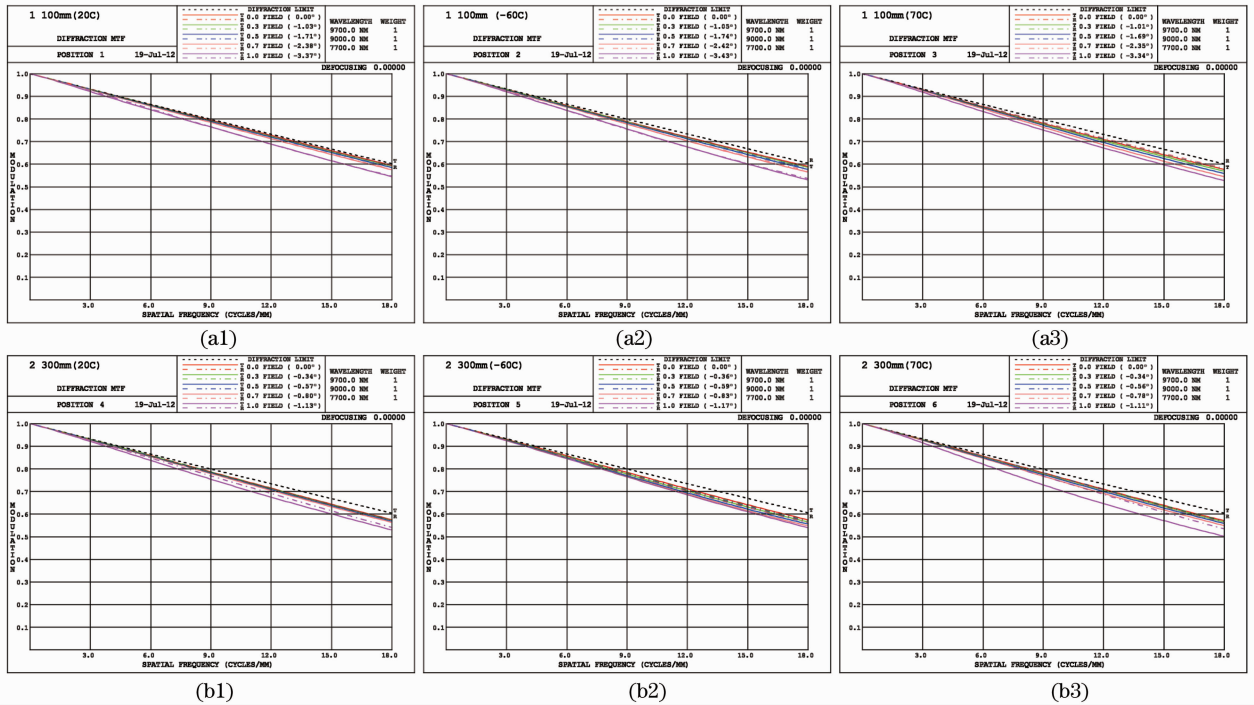


Fig. 2 MTF curves of the optical system at $20 \text{ }^\circ\text{C}$, $-60 \text{ }^\circ\text{C}$ and $70 \text{ }^\circ\text{C}$ for the focal length of (a1)~(a3) 100 mm and (b1)~(b3) 300 mm

Table 3 shows the spot diagram of the system. The maximum root-mean-square (RMS) radius is about $19.6 \text{ } \mu\text{m}$. The RMS radius is smaller than the Airy radius and the pitch of detector.

The MTF, diffraction encircled energy, and spot diagram show an excellent imaging performance. The structure of the system is very compact. These make it adaptable to space camera systems and also prove that the optical passive method is correct and useful in the design of infrared optical system.

Table 3 Spot diameter of the optical system

FOV / (°)	RMS radius for EFL of 100 mm / μm			FOV / (°)	RMS radius for EFL of 300 mm / μm		
	20 °C	-60 °C	70 °C		20 °C	-60 °C	70 °C
0	9.7	12.4	13.1	0	5.4	12.4	11.8
2.1	9.8	13.5	11.9	0.6	6.7	13.4	12.1
3.4	10.0	14.6	11.1	1.0	8.4	15.7	12.4
4.8	10.6	15.1	11.8	1.4	10.5	16.1	13.1
6.7	16.7	16.7	18.7	2.0	16.2	19.5	19.6

4 Conclusion

We have discussed a dual-field-of-view long wavelength infrared optical system. The optical layout is compact and does not need operational focusing adjustment. Color correction and athermalization are obtained by appropriate choice of optical materials (without diffractive surfaces). The cost of the space camera is reduced by means of passive athermalization and low sensitive tolerances.

References

- Allen Mann. Infrared Optics and Zoom Lenses [M]. Bellingham: SPIE Press, 2009
- Warren J. Smith. Modern Optical Engineering, the Design of Optical Systems [M]. Bellingham: SPIE Press, 2008
- Chen Xiao, Yang Jianfeng, Ma Xiaolong *et al.*. Athermalization design of wide temperature range for hybrid refractive-diffractive objective in 8~12 μm [J]. *Acta Optica Sinica*, 2010, **30**(7): 2089~2092
陈 潇, 杨建峰, 马小龙 等. 8~12 μm 折-衍混合物镜超宽温度消热差设计[J]. *光学学报*, 2010, **30**(7): 2089~2092
- Liu Lin, Shen Weimin, Zhou Jiankang. Design on athermalised middle wavelength infrared optical system with large relative aperture [J]. *Chinese J. Lasers*, 2010, **37**(3): 675~679
刘 琳, 沈为民, 周建康. 中波红外大相对孔径消热差光学系统的设计[J]. *中国激光*, 2010, **37**(3): 675~679
- Cen Zhaofeng, Li Xiaotong. Optical system thermal effect analysis and athermal design [J]. *Laser & Optoelectronics Progress*, 2009, **46**(2): 63~67
岑兆丰, 李晓彤. 光学系统温度效应分析和无热化设计[J]. *激光与光电子学进展*, 2009, **46**(2): 63~67
- Hu Yuxi, Zhou Shaoxiang, Xiangli bin *et al.*. Design of athermal optical system [J]. *Acta Optica Sinica*, 2000, **20**(10): 1386~1391
胡玉禧, 周绍祥, 相里斌 等. 消热差光学系统设计[J]. *光学学报*, 2000, **20**(10): 1386~1391
- Guo Yonghong, Shen Mangzuo, Lu Zukang. Athermal design for infrared diffractive/refractive optical system [J]. *Acta Optica Sinica*, 2000, **20**(10): 1392~1394
郭永洪, 沈忙作, 陆祖康. 折射/衍射红外光学系统的消热差设计[J]. *光学学报*, 2000, **20**(10): 1392~1394
- L. Rayces, L. Lebich. Thermal compensation of infrared achromatic objectives with three optical materials [C]. *SPIE*, 1990, **1354**: 752~759
- Yasuhisa Tamagawa, Satoshi Wakabayashi, Toru Tajime. New design method for athermalized optical systems [C]. *SPIE*, 1992, **1752**: 232~238
- Yasuhisa Tamagawa, Satoshi Wakabayashi, Toru Tajime *et al.*. Multilens design with an athermal chart [J]. *Appl. Opt.*, 1994, **33**(34): 8009~8013